Vienna Congress on Recent Advances in
Earthquake Engineering and Structural Dynamics 2013 (VEESD 2013)
C. Adam, R. Heuer, W. Lenhardt & C. Schranz (eds)
28-30 August 2013, Vienna, Austria
Paper No. 243

Experimental tests on the seismic behaviour of unreinforced load-bearing masonry structures

C. Mordant[1], M. Dietz[2], H. Degée[1]

[1] Department of Architecture, Geology, Environment and Construction, University of Liège, Liège, Belgium
[2] Department of Civil Engineering , University of Bristol, Bristol, UK

Abstract. The paper describes recent experimental shaking table tests carried out on load-bearing unreinforced masonry shear walls in earthquake conditions, within the European research project SERIES. The first phase of the experimental activity investigates the response of four simple unreinforced masonry walls, two of them including rubber acoustic isolation devices. The second phase deals with the testing of specimens with T- and L-shaped walls (shear wall with flanges) coupled at their top by a concrete lintel and a prefabricated concrete slab. The paper summarizes interesting results obtained on the general behaviour of the walls, on the estimation of equivalent elastic and shear moduli, on the influence of the soundproofing devices and on the global frame behaviour of the system.

Keywords: Unreinforced masonry, Shaking table, Tensile/shear moduli, Acoustic devices, Frame behaviour.

1 INTRODUCTION

1.1 General context

Traditionally, the design of masonry buildings and, in particular, of unreinforced load-bearing masonry structures concerns family houses and is left under the responsibility of the architect with no or limited engineering. The past two decades have however seen an increasing interest of engineers in this field and led to improvements in the knowledge and design of such structures. Moreover, thanks to better mechanical properties of the materials and to an improved control of the global structural behaviour, the range of application has been extended to multi-storey buildings up to 5-6 levels (Stuerz, 2012).

When these buildings are used for apartments, high soundproofing performances are required to fulfil the most recent standards in terms of individual comfort. A possible and rather widely spread solution consists in placing a rubber layer at the top and/or bottom of each wall to prevent acoustic bridges, as shown in **Figure 1**, where the black layer below the bricks is actually a 1 cm thick rubber layer implemented for acoustic reasons. The influence of such a solution on the global seismic behaviour of multi-storey unreinforced masonry structures optimized for acoustic performances is however questionable, even in the case of moderate seismic action. Indeed, the rubber layers are likely to modify the stiffness and resistance of the structural elements as well as the boundary conditions of the walls. In this perspective, shaking table tests have been carried out at the Earthquake and Large Structures Laboratory (EQUALS) of the University of Bristol, in the framework of the European project SERIES. The MAID research program actually includes two phases, where the first one mainly aims at investigating the effects of the acoustic devices. To this purpose, the seismic response of four simple unreinforced clay masonry walls is studied, two of them including acoustic isolation rubber layers at their bottom and top.

Figure 1. Acoustic solution (Wienerberger)

Beside the investigation specifically targeting the acoustic devices, the MAID testing program also covers a second phase not directly related to these acoustic elements. In this second phase, two additional specimens are tested, i.e. a frame with two T-shaped walls and a second one with L-shaped walls ("flanged" shear walls), in both cases coupled by a concrete lintel and a concrete slab. A detailed description of the corresponding test specimens is given in section 3. This second part of the project is focused on the contribution of the parts of the structural elements perpendicular to the earthquake direction and on the characterization of the frame behaviour.

This paper presents a general overview of the test specimens, procedures and results of the two phases. For the first phase, a comparison of the actual experimental behaviour with respect to a simple cantilever beam model is also performed with the objective of getting estimates of the main material characteristics.

2 SINGLE WALLS DYNAMIC TESTS

2.1 Description of the specimens

The specimens of the first phase consist in four single walls constituted by thin-bed layered clay masonry with empty vertical joints (see **Figure 2**). Two of them are characterized by an aspect ratio close to 1, while the aspect ratio is close to 0.4 for the other two. One wall of each aspect ratio has rubber layers at its bottom and top. Exact dimensions of the walls are the following:

- $length\ x\ height\ x\ width\ =\ 2.1\ m\ x\ 1.8\ m\ x\ 0.138\ m$ (long wall);
- $length\ x\ height\ x\ width\ =\ 0.72\ m\ x\ 1.8\ m\ x\ 0.138\ m$ (short wall).

The block dimensions used for all specimens are:

- $length\ x\ height\ x\ width\ =\ 300.0\ mm\ x\ 188.0\ mm\ x\ 138\ mm$

Mechanical characteristics of the units and masonry are as follows:

- Normalised compressive strength of units (EN 772-1 Annex A): $f_b = 13.0\ N/mm^2$
- Measured characteristic masonry compressive strength (EN 1052-1): $f_k = 5.6\ N/mm^2$
- Characteristic compressive strength (NBN-EN 1996-1-1): $f_k = 3.9\ N/mm^2$

An additional mass of 5 tons is located on the top of the walls to emulate the structural floor load, with due consideration for the shaking table payload and for the common range of compression level in masonry structures. Details of the specimens and test information are extensively described in (Mordant, 2012), (Mordant et al., 2013a) and (Degée et al., 2013)

Figure 2. General view of a specimen (long wall)

2.2 Testing procedure

Two types of tests are alternatively carried out during the experimental procedure. The aim of the first tests type is to characterize the dynamic properties of the specimens (modal shapes, natural frequencies, damping ratio). It consists in submitting the wall to a white noise random excitation at a low acceleration level. The second type is the seismic testing *stricto sensu* based on an artificially generated seismic input consistent with Eurocode 8 spectrum.

In practice, each specimen is first submitted to a "white noise" test to determine its initial dynamic properties. The experimental procedure is then composed of an alternation of seismic tests, with an acceleration level increased step-by-step, and "white noise" tests in order to study the effects of the earthquake action on the dynamic properties of the specimen. The maximal accelerations recorded during the seismic tests S01 to S09 are given in **Table 1**. Details of the testing procedures and analysis of the results are available in (Mordant, 2012) and (Degée et al., 2013).

Table 1. Maximal Accelerations (in *g*)

Test number	S01	S02	S03	S04	S05	S06	S07	S08	S09
	g	g	g	g	g	g	g	g	g
Long wall without rubber	0.039	0.078	0.078	0.158	0.238	0.323	0.450	0.572	0.688
Long wall with rubber	0.043	0.090	0.088	0.187	0.278	0.356	0.457	0.569	0.639
Short wall without rubber	0.041	0.065	0.064	0.087	0.136	0.133	0.178	0.187	0.234
Short wall with rubber	0.042	0.060	0.061	0.080	0.124	0.128	0.171	/	/

2.3 Tests results

This paper provides only a summary of the main information drawn at this stage from the test observations and presents their main conclusions. It is however to be highlighted that additional model calibrations and consequent further exploitations of the test results are still in progress.

1. Identification "white noise" tests show a clear difference in terms of natural frequencies between walls exhibiting a same aspect ratio but including rubber layers or not. A drop of about 30% to 40% is observed in presence of rubber layers for undamaged situations. A progressive decrease of the natural frequencies and an increase of the damping ratio are also observed when the acceleration level increases, associated with the progressive deterioration of the specimens and in particular of their connection with their foundation. These variations are however less pronounced for the walls with rubber, showing a lower damaging of the wall-foundation connection for a same ground acceleration level. Graphical illustrations of these observations are given in **Figure 3** for the long walls.

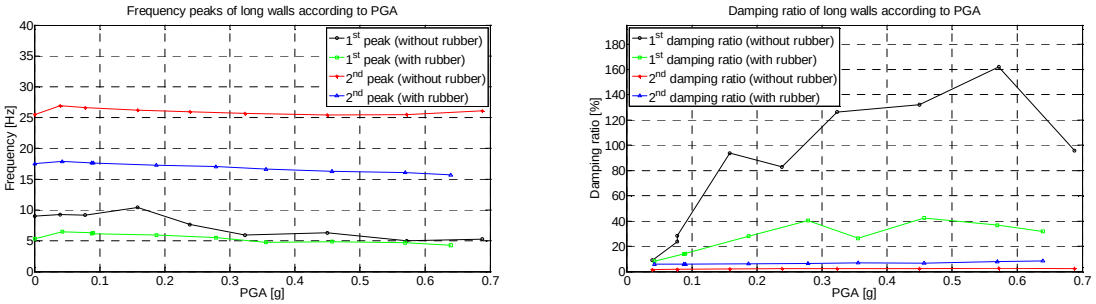

Figure 3. Evolution of natural frequencies and damping ratio of the long walls

Although the presence of rubber could be at first considered as negative (higher flexibility and larger displacements), the results show a possible benefit in the use of rubber layers at walls extremities since the degradation of the dynamic properties is less affected by the earthquake action. A possible and convenient explanation is proposed in (Mordant et al., 2013a) and assumes that the dynamic behaviour is actually changed in presence of acoustic devices, switching from a discontinuous rocking behaviour to a smoother classical bending.

2. A very relevant quantitative information taken from the seismic tests consists in the measurement of the compressive length (i.e. contact length between the wall and its foundation), knowing that this length is a major necessary data to perform the strength verification according to the Eurocodes. The evolution of the compressive length with respect to the acceleration level is provided in **Figure 4**. This figure shows a favourable influence of the rubber devices on the compressive length since this latter is larger for the same acceleration level in presence of acoustic insulation devices. Comparison between measurements and theoretical predictions is carried out and yields the conclusion that the theoretical calculation is relevant for low levels of acceleration, but underestimates the compressive length when the acceleration level becomes higher.

3. As proposed in (Mordant et al., 2013b), the observed dynamic behaviour during the seismic sequences can be sorted in three groups, on the base of the comparison of the rotations measured at the bottom and top of the wall. (i) The first group gathers the seismic tests at a low acceleration level, where a significant difference between rotations at the wall extremities is observed (see **Figure 5**, left). Among the set of experimental results elaborated during the MAID project, this group includes the first three tests for both the long and short walls (S01, S02 and S03). Section 2.4 of this paper will focus specifically on the modelling of this situation that can reasonably be modelled assuming that the wall is a cantilever fully clamped in its foundation. This range of acceleration and the associated modelling assumptions are mainly useful for assessing damage limit states at low acceleration level. (ii) The second group corresponds to tests where quasi-equal rotations are measured at the bottom and top of the wall (see **Figure 5**, right). This behaviour is observed when the acceleration level is rather high (S07, S08 and S09) and can be reasonably described by a model assuming a rocking of the wall considered as a rigid body.

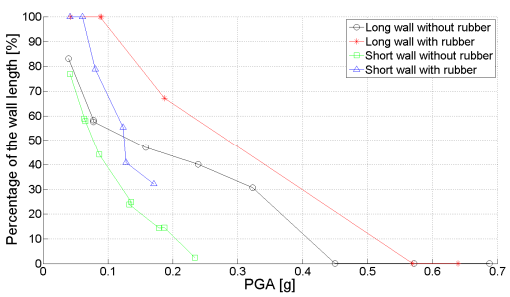

Figure 4. Evolution of the compressive length according to PGA (in percentage of the total wall length)

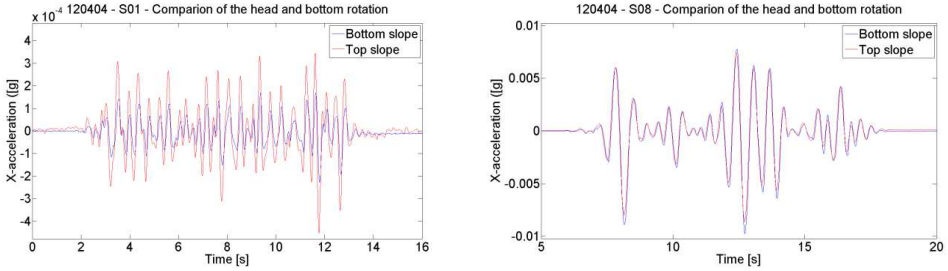

Figure 5. Comparison of the head and bottom rotation – short wall without rubber

Comparisons between measurements and modelling are provided in (Mordant et al., 2013b).This range is of prime interest for the evaluation of the ultimate limit state. (iii) The third group comprises all the intermediate situations and corresponds to tests with an intermediate acceleration level (here S04, S05 and S06). A proper modelling would thus require combining a simple cantilever with a rocking model. It is felt however of a more limited practical interest.

2.4 Theoretical model for low intensity earthquake shakes

The theoretical model developed here is based on the Timoshenko beam theory (Timoshenko, 1939). In this theory, the equations of motions are given by a set of two uncoupled equations (1) and (2) under the assumption of a linear elastic, isotropic and homogeneous beam with a constant cross-section:

$$EI.\frac{\partial^4 y(x,t)}{\partial x^4} - \left(\rho I + \frac{\rho EI}{k\prime G}\right)\frac{\partial^4 y(x,t)}{\partial x^2 \partial t^2} + \rho A\frac{\partial^2 y(x,t)}{\partial t^2} + \frac{\rho^2 I}{k\prime G}\frac{\partial^4 y(x,t)}{\partial t^4} = 0 \quad (1)$$

$$EI.\frac{\partial^4 \alpha(x,t)}{\partial x^4} - \left(\rho I + \frac{\rho EI}{k\prime G}\right)\frac{\partial^4 \alpha(x,t)}{\partial x^2 \partial t^2} + \rho A\frac{\partial^2 \alpha(x,t)}{\partial t^2} + \frac{\rho^2 I}{k\prime G}\frac{\partial^4 \alpha(x,t)}{\partial t^4} = 0 \quad (2)$$

where $y[m]$ is the transverse displacement and $\alpha[rad]$ is the angle of rotation due to bending. These variables are function of the axial coordinate of the beam $x[m]$ and of the time $t[s]$. The others parameters are the cross-section area $A[m^2]$, the inertia $I[m^4]$, the tensile modulus $E[N/m^2]$, the shear modulus $G[N/m^2]$, the density $\rho[kg/m^3]$ and the shape factor $k'[-]$ (i.e. the ratio between the full cross-section and the reduced cross-section used for evaluating the shear stiffness of the beam, typically equal to 5/6 for rectangular cross-sections).

The variables of the equations (1) and (2) can be expressed in a modal base thanks to the change of variables given in equations. (3) and (4).

$$y(x,t) = \phi(x).e^{i\omega t} \quad (3)$$

$$\alpha(x,t) = \psi(x).e^{i\omega t} \quad (4)$$

This leads to equations (5) and (6).

$$EI.\phi''''(x).e^{i\omega t} + \left(\rho I + \frac{\rho EI}{k'G}\right)\phi''(x).\omega^2 e^{i\omega t} - \rho A\phi''(x).\omega^2 e^{i\omega t} + \frac{\rho^2 I}{k\prime G}\phi(x).\omega^4 e^{i\omega t} = 0 \quad (5)$$

$$EI.\psi''''(x).e^{i\omega t} + \left(\rho I + \frac{\rho EI}{k'G}\right)\psi''(x).\omega^2 e^{i\omega t} - \rho A\psi''(x).\omega^2 e^{i\omega t} + \frac{\rho^2 I}{k\prime G}\psi(x).\omega^4 e^{i\omega t} = 0 \quad (6)$$

These last two equations are solved as differential equations of the fourth order with constant coefficients and result in the spatial solutions of Eqs. (5) and (6). Details of the method and solutions are described, for instance, in (Han at al., 1999). These general spatial solutions involve four parameters to be determined according to the boundary conditions of the beam.

In the case of the present experimental test conditions, for the low acceleration levels (test results of group 1 according to the classification proposed in the previous section), the specimens can reasonably be considered as cantilever beams. Therefore, the top end is free while the bottom end can be considered as clamped. The boundary conditions are then given by (7) for the free end and by (8) for the clamped end:

$$\frac{\partial \alpha}{\partial x} = 0 \text{ and } k'GA\left(\frac{\partial y}{\partial x} - \alpha\right) = 0 \tag{7}$$

$$\alpha = 0 \text{ and } y = 0 \tag{8}$$

Eqs. (7) and (8) result in a system of four equations with four unknowns whose determinant has to be equal to zero to allow a solution different from the trivial one with all unknowns equal to zero. When matching the determinant with zero, the frequency equation can be derived. The roots of this latter are the natural frequencies of the beam. For instance, the frequency equation of a cantilever beam is given by (10):

$$(a^2 - b^2)\sin aL \sinh bL - ab\frac{a^4+\gamma^4a^4+4\gamma^2a^2b^2+\gamma^4b^4+b^4}{(a^2+\gamma^2b^2)(b^2+\gamma^2a^2)}\cos aL \cosh bL - 2ab = 0 \tag{10}$$

where $a, b[m^{-1}]$ are the wave numbers and $\gamma[-]$ is equal to $2(1+\nu)/k'$ where ν is the Poisson's ratio. The wave numbers are obtained as the roots of the characteristic equations of Eqs. (5) or (6). In the equation (10), a is an imaginary number and b is a real one (although b can in the most general case be also imaginary). All the possibilities are developed in (Han at al., 1999).

A major difference is however identified between the assumptions leading to the above mathematical methodology and the actual experimental conditions of the MAID tests. This difference is related to the presence of a significant additional concentrated mass lying at the top of the wall. Indeed, although the characteristic equation is the same, the boundary conditions at the free end must be modified to account for the shear stresses induced by the inertial forces associated with this concentrated mass, according to Eq. (11).

$$\frac{\partial \alpha}{\partial x} = 0 \text{ and } k'GA\left(\frac{\partial y}{\partial x} - \alpha\right) = -T(x,t) = -Mass.\frac{\partial^2 y}{\partial t^2} = Mass.\phi(x).\omega^2 e^{i\omega t} \tag{11}$$

Hence, the presence of the mass modifies the frequency equation, which becomes (12):

$$(a^2 - b^2)\sin aL \sinh bL - ab\frac{a^4+\gamma^4a^4+4\gamma^2a^2b^2+\gamma^4b^4+b^4}{(a^2+\gamma^2b^2)(b^2+\gamma^2a^2)}\cos aL \cosh bL - 2ab + \frac{Mass.\omega^2}{k'GA}\frac{(a^2+b^2)}{(a^2-b^2)}\frac{(1+\gamma^2)^2}{\gamma^2}\left[\frac{a^2b}{(b^2+\gamma^2a^2)}\sin aL \cosh bL - \frac{ab^2}{(a^2+\gamma^2b^2)}\sinh bL \cos aL\right] = 0 \tag{12}$$

The roots of equation (12) provide the natural frequencies of the beam representing the specimens without rubber with an additional mass placed at the top.

2.5 Comparisons with tests results

The theoretical model described above on the base of the Timoshenko theory leads to the frequency equation (12) from which the theoretical natural frequencies can be deduced. On the other hand, the natural frequencies have been identified during the tests from white noise excitations. Details of the post-processing procedure are given in (Mordant, 2012). These identifications results are given in **Table 2** for the seismic tests of the first group. Only the first natural frequency is considered for the comparison.

Table 2. Measured first natural frequency

Test number	S01	S02	S03	S04	S05	S06
	Hz	Hz	Hz	Hz	Hz	Hz
Long wall without rubber	9.33	9.21	9.18	9.78	9.04	6.8
Short wall without rubber	3.89	3.95	3.79	3.79	/	/

Equation (12) is actually a function of two variables, namely the two wave numbers. These latter depend on geometrical and material parameters (area, inertia, masses) on the one hand and mechanical ones (tensile and shear modulus) on the other hand. The geometrical parameters are clearly identified from the specimen geometry. However the mechanical properties to be used for a masonry wall subjected to combined in-plane bending and shear are more questionable. As a preliminary guess, reference can be made to Eurocode recommendations (Eurocode, 2004). It is then advised to consider a value of 500 times the characteristic compressive strength for the elastic modulus – actually 1000 f_k according to Eurocode 6, divided by two to account for the cracking in seismic situation – and the shear modulus should be taken as 40% of the elastic modulus.

These two assumptions are assessed by varying the elastic modulus and the elastic-to-shear modulus ratio in the analytical approach in such a way to reach the measured value of the natural frequency. The range of variation of the material parameters is chosen in a reasonable physical domain. The mapping of the results is presented for the short and long walls respectively in **Figure 6.a** and **b** and shows that a fitting of the theoretical frequency with respect to the measured frequency can be obtained for various combinations of E and G.

The results for the short wall show a rather limited interval of variation of the elastic modulus, whatever the assumed value of the G/E ratio and even for progressively damaged specimens. The values range from 350 to 550 f_k. If considering the code recommended value of the elastic to shear modulus ratio G/E, the corresponding tensile modulus is about 450 f_k in the initial situation. For increasing values of the acceleration level and hence for progressively degrading material, decreasing values of the elastic modulus are also necessary to make the analytical model fit with the test measurements. With regard to the G/E ratio, the rather vertical orientation of the curves in **Figure 6.a** is the sign of a limited influence of the assumption on this ratio on the outcome of the analytical model. This was indeed expected according to the limited contribution of the shear deformability with respect to the bending deformability in the case of the short wall (about 10 %), as shown in **Table 3**. As a conclusion, in the case of the short wall, Eurocode recommendations seem convenient regarding the G/E ratio, but slightly overestimate the elastic modulus to be used for the calculation of the dynamic characteristics of the wall.

Table 3. Bending and shear deformability

	Bending deformability	Shear deformability
	m/N	m/N
Long wall	$9{,}3607\,.\,10^{-9}$	$9{,}5557\,.\,10^{-9}$
Short wall	$2{,}3226\,.\,10^{-7}$	$2.7871\,.\,10^{-8}$

Applying the same approach to the long wall leads to a larger range of possible values for the elastic modulus, from 150 to 500 f_k. Moreover, the cross-effect of the E and G values in the fitting procedure of the frequency is more pronounced in this case (the higher the G, the smaller the E and vice-versa), contrary to the case of the short wall where the value of E is by far less depending on the value of G. This was indeed expected since bending and shear deformability are of the same order of magnitude, as shown in **Table 3**. With the code recommended value for the G/E ratio (0.4), the elastic

modulus starts from 200 f_k and decreases down to 150 f_k for progressively damaged situations. This recommended value of G/E is however questionable. Indeed on the one hand, it implies the combined use of unrealistically low values of the elastic modulus, while on the other hand, for a wall with open vertical joints, the shear deformability is most likely higher than for classical masonry. Therefore smaller values of the shear modulus should be considered. For instance, if considering G/E equal to 0.2, the corresponding elastic modulus is about $300 f_k$, which looks more reasonable. A last comment has to be made regarding the seismic test 6. Indeed, **Figure 6.b** shows a large difference between results for this test with respect to all the previous ones. The difference could be justified by a change in the global behaviour of the wall. From the sixth test, the rocking effect becomes indeed predominant, resulting in increased degradation of the connection of the wall with its foundation and therefore in a localized reduction of the mechanical properties of the system. This effect cannot be taken into consideration with the proposed model for which mechanical properties are assumed constant all over the wall. This issue will be further studied in the future in parallel with the accounting for the presence of the rubber layer.

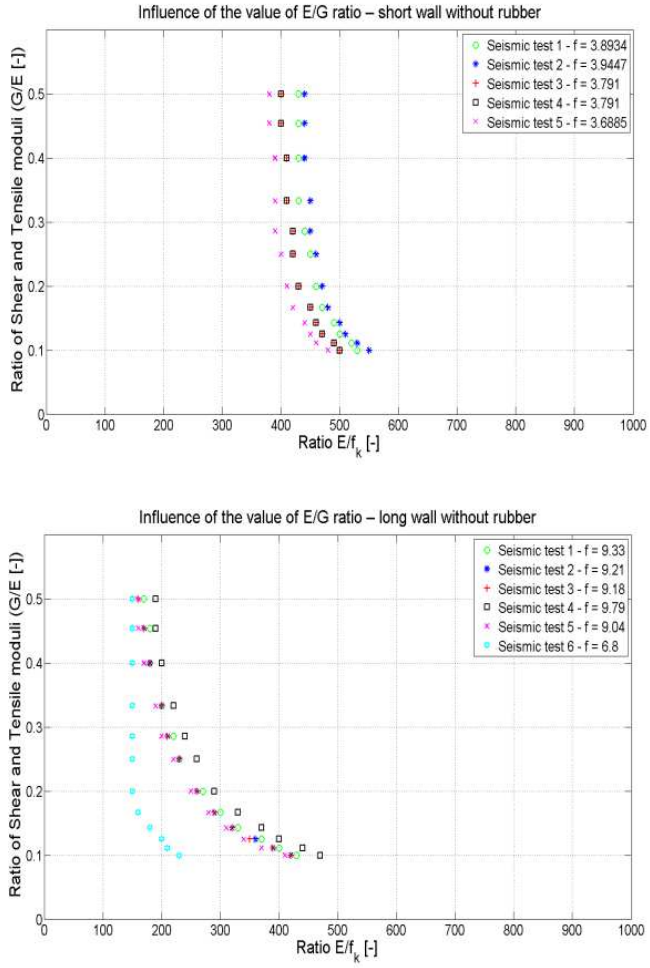

Figure 6. Influence of the E/G ratio. (a) Short wall – (b) Long wall.

3 FRAME TESTS

The specimens of the second phase are two frames with T-or L-shaped walls as piers, linked together by a concrete lintel. The first specimen of the second phase is a frame with T-shaped walls, oriented asymmetrically (see **Figure 7**, left). This configuration was chosen in order to study the effects of a global torsion. The second specimen is a frame with L-shaped walls (see **Figure 7**, right). For this second specimen, a different connection system is used for each of the two piers of the frame. The first one is built with a classical masonry scheme for edges, i.e. alternation of the units layers, while the other has its flange (wall perpendicular to the frame plan) glued to its "shear wall" (wall in the plan of the frame) without interlocking of the units. The testing procedure for this second phase follows the same outline as the first one (alternation of white noise identifications and seismic tests with increasing intensity). White noise characterization of the specimens is systematically carried out for the two directions (along and perpendicular to the frame). The seismic tests for each specimen are as well alternatively carried out in the two directions and then increased.

Figure 7. General view of the specimens of the second phase

The first frame (i.e. with T-shaped piers) is loaded by a concrete slab resting on the entire system. Shear walls and flanges are thus submitted to a same pre-compression level under gravity load. For the second frame (i.e. with L-shaped piers), two different gravity load cases are tested. First, the slab is placed so as to get walls equally loaded (as for the first frame). A second set of tests is then carried out with the slab resting only on the flanges, this second situation corresponding to a slab spanning in one direction only. The range of acceleration of these three sets were [0.05 g; 0.47 g], [0.05 g; 0.18 g] and [0.05 g; 0.20 g] respectively.

Different collapse mechanisms were observed. The tests on the T-shaped frame were stopped because of excessive damage in the piers due to the large displacements induced by the torsional effects. Regarding the L-shaped frame, a significant rocking behaviour was observed for the first loading case. Tests were stopped in purpose before reaching significant damage, although higher acceleration level could certainly have been reached, in order to allow testing a second load case. For this second load case, tests were stopped after the failure of the vertical intersection line between the shear wall and the flange for the pier built in a traditional way (interlocked masonry).

Results of the second phase are not entirely processed at the time of finalizing the present paper and will thus be detailed in further publications to come. Processing and analysis of these results will focus on the frame effect and on the contribution of the walls perpendicular to the earthquake action since these effects remain rather poorly controlled by the current design methodologies, in spite of recent studies showing their positive impact on the seismic strength of masonry structures (Milani et al., 2009).

4 CONCLUSIONS

The paper summarizes the results of shaking table tests on simple unreinforced masonry structures.

- In the first part, the paper describes the general observations on single wall specimens, including the consequences of the use of rubber elements on the global behaviour, in terms of rocking effects and of progressive damage of the system.
- The second part focuses on the tests with low acceleration levels and presents a modelling of the specimens without rubber with the objective of calibrating the elastic and shear moduli. The following observations are made:
    - For the short wall, the value of the elastic modulus recommended by the standards seems to be slightly overestimated, while the impact of uncertainties about the shear modulus on the estimated frequency is not significant.
    - For the long wall, the influence of the G/E ratio is more important because of the higher dependency of the frequency on the shear deformability. Results indicate that this ratio should be less than the classically recommended value of 0.4, possibly because of the presence of empty vertical joints.
- The third part briefly introduces the specimens and the test procedure of the second phase of the MAID project and highlights the main issues on which the processing of the results is focused. Results are expected to provide information about the frame behaviour of masonry structures and about the contribution of walls perpendicular to the earthquake direction.

Short-term perspectives also cover additional investigations on the behaviour and modelling of walls with rubber layers. The final objective is the full integration of structural models to study entire buildings.

ACKNOWLEDGEMENTS

The research leading to these results has received funding from the European Union Seventh Framework Programme (FP7/2007-2013) under grant agreement n° 227887, SERIES. H. Degée also acknowledges the direct support received from F.R.S.-FNRS (Belgian Fund for Research).

REFERENCES

Degée, H. et al., (2013). MAID - Seismic behaviour of L and T-shaped unreinforced Masonry shear walls including Acoustic Insulation Devices, FP7 SERIES program, TA User group 5, Final Report.

Eurocode 6, (2004). Seismic Design of masonry structures – Part 1.1 : Common rules for reinforced and unreinforced masonry structures.

Han, S.M., Benaroya, H. and Wei, T. (1999). Dynamics of transversely vibrating beams using four engineering theories. *Journal of Sound and Vibration*, **225**(5):935-988.

Milani, G., Beyer, K. and Dazio,A. (2009). Upper bound limit analysis of meso-mechanical spandrel models for the pushover analysis of 2D masonry frames. *Engineering Structures*, **31**:2696-2710.

Mordant, C. (2012). Contribution to experimental tests on the seismic behaviour of masonry structural elements. *Master dissertation*, University of Liège.

Mordant, C., Dietz, M. and Degée, H. (2013a). Seismic behaviour of thin-bed layered unreinforced clay masonry shear walls including soundproofing elements. In: Alper Ilki and Michael N. Fardis (eds), *Proc SERIES Workshop. Geotechnical, Geological and Earthquake Engineering series (chapter 6).* (in press)

Mordant, C., Dietz, M. and Degée, H. (2013b). Shaking table tests on unreinforced load-bearing masonry walls – comparison with simple rocking models. In: M. Papadrakakis, V. Papadopoulos, V. Plevris (eds.), *Proc. 4th ECCOMAS Thematic Conference on Computational Methods in Structural Dynamics and Earthquake Engineering (COMPDYN 2013)*; June 12-14, 2013, Kos Island, Greece. (to be published)

Timoshenko, S. (1939). *Théorie des vibrations*. Paris et Liège, libraire polytechnique Ch. Béranger.